Integrating AI and sustainable materials: machine learning approaches to wood structural behavior

M. González-Palacio[1,*], JM. García-Giraldo[2] and L. González-Palacio[3]

[1]Universidad de Medellín, Faculty of Engineering, Department of Computer Science, Carrera 84 #30-65, CO 050026 Medellín, Colombia
[2]Universidad de Medellín, Faculty of Engineering, Department of Civil Engineering, Carrera 84 #30-65, CO 050026 Medellín, Colombia
[3]Universidad EAFIT, Faculty of Engineering, Department of Computer Science, Carrera 49 N° 7 Sur - 50, CO 050022 Medellín, Colombia
[*]magonzalez@udemedellin.edu.co

Abstract. Wood is a potential construction material that provides a renewable source for this crucial task compared to other classical materials, such as steel or concrete, with high carbon fingerprinting levels. This suitable material minimizes energy use and adds more sustainability to ecological consciousness. Tree planting promotes the balance of the carbon dioxide ecosystem and captures and stores greenhouse gas emissions. Wood also has peculiar characteristics in terms of its structural strength and thermal insulation, optimizing energy consumption by reducing the need for cooling or heating needs. To use this material in construction, it is mandatory to study the resistance parameters like compressive, tensile, and shear strengths, enabling it for great-span structural projects. The traditional modeling strategies used for characterizing stress-strain performances usually simplify the assumptions, overpassing the complex mechanical behavior of the wood under different physical conditions. Nonetheless, previous analyses have shown that the traditional models may exhibit significant deviations from the actual resistance parameters since they can be limited in predicting non-linear and anisotropic properties inherent in wood. To address these limitations, this study proposes using machine-learning-based regressors to predict the mechanical properties of wood. Notably, we propose Multiple Linear Regression models to preserve the model's interpretability while preserving the ability to model the linear properties in the studied scenarios. Furthermore, we use metaheuristic models based on deep learning and ensemble methods to increase the goodness of fit of the predictions. We used an experimental campaign with a widespread type of wood characterization of different parameters under tension parallel to the grain, compression parallel and perpendicular to the grain, and shear conditions. The results showed a lower root mean square error (RMSE) and a higher determination index (R^2). Preliminary results demonstrated the ability of machine-learning-based modeling to obtain more accurate and reliable mechanical behavior of renewable construction materials like wood.

Key words: artificial neural networks, machine learning, random forest, sustainable materials.

INTRODUCTION

A challenge for the global construction industry is related to the growing infrastructure requirements that cause minimal environmental degradation. The sector is responsible for 37% of total global CO_2 emissions and plays a critical role in contributing to climate change (Ding et al., 2022). To achieve this, it is necessary to use more sustainable, cost-effective, high-performance materials (Kumar et al., 2023) using the tools provided by Industry 4.0 (Giraldo & Palacio, 2020), such as the Internet of Things (Palacio et al., 2017; Gonzalez-Palacio et al., 2018), and Artificial Intelligence (AI) (Kim et al., 2024). However, the study of these materials has been mainly based on concrete and steel that have formed the backbone of construction over many years, and their environmental impacts, such as carbon footprint and resource depletion, have scarcely been studied using cutting-edge AI-based tools (Rane, 2023).

In that way, researchers continue searching for alternative materials that would serve in a more sustainable direction using the paradigms of Industry 4.0. Among them, wood is one of the alternatives that presents the advantage of renewal, carbon sequestration, and mechanical properties comparable to traditional materials in many uses (Peng et al., 2023). Wood is one of the few construction materials that requires low energy consumption, resulting in lower CO_2 emissions during production. Its versatility enables shorter construction times and reduces the need for specialized tools while providing an aesthetically pleasing appearance with an attractive visual design (Rodríguez-Grau et al., 2022). Despite such favorable factors, complete structural characterization of wood regarding mechanical resistance parameters, i.e., compressive, tensile, and shear strengths, remains a significant challenge. This is a limitation in the wide acceptability of wood for structural purposes, where there is a necessity for reliability and predictability of mechanical performance.

Traditional methods for characterizing wood's mechanical properties rely on extensive experimental testing, which can be time-consuming and costly. Standardized testing procedures have used different recommendations to characterize the wood performance for construction, like those provided by the American Society for Testing and Materials and the International Organization for Standardization (ASTM, 2021), which demand large samples and special instruments in harsh environments with unfavorable conditions (M. González-Palacio et al., 2024) to measure all the resistance parameters of wood accurately. Many tests involve destructive procedures, resulting in material loss and higher research expenses. Besides, the need for competent personnel and extreme testing conditions may also raise the cost and duration of the characterization studies. Hence, there is an increasing interest in alternative approaches that can efficiently predict the mechanical properties of wood with a few experimental inputs.

Several studies have explored different methodologies for modeling and predicting the mechanical properties of wood materials. Particular research efforts have been directed toward developing empirical models and advanced computational techniques to understand the relationships between different mechanical parameters better. Unlike materials such as steel and concrete, which have numerous studies on their mechanical properties and the correlations between them, wood has a more limited number of studies aimed at determining its mechanical properties (Arriaga et al., 2023). This limited

information is primarily due to the wide variety of structural wood species used in the construction sector and the significant variability in mechanical properties among wood species across different production regions worldwide.

However, some open issues are a matter of research nowadays. A crucial gap concerns diminishing the number of experiments performed to characterize the wood performance under different conditions. The current methodologies require large datasets containing stress and strain data, which demand extensive measurement campaigns. Thus, the current study fills this gap by introducing a novel methodology that uses parallel-to-the-grain stresses and strains to forecast perpendicular-to-the-grain stress using Machine Learning (ML) strategies, aiming to diminish the need for performing extensive measurement campaigns in different directions to characterize the wood behavior. The contributions of this research are threefold:

1. We analyze variable correlations among the predictors to find relations between parallel and perpendicular grain stresses and strain.

2. We model these relationships using different parametric and nonparametric strategies like Multiple Linear Regression (MLR) (Yan & Su, 2009), Artificial Neural Network (ANN) (Kim et al., 2024), and Random Forest (RF) (Sharma et al., 2024) using only a minimum experimental dataset required for wood property prediction.

3. We improve the accuracy of the predictions using RF models that yield an R^2 up to 0.91 for the elastic and inelastic regions. The R^2 was obtained from the test set once we randomly split the database into training and test sets. We used the training set to tune different hyperparameters according to the chosen methods, and the test set was used to measure the ability of the trained methods to generalize the results since this particular subset was unknown for the method in the training phase. Thus, we computed the R^2 using the actual measured values from the test set and the forecasted values using our models. As a consequence, we show that machine learning algorithms effectively enhance predictive accuracy performance.

The rest of this paper is organized as follows: Section II establishes the theoretical foundations that support the research problem addressed in this study. Section III describes the database used and provides insights about the collected data. Section IV provides the methodology to fit diverse machine-learning-based models from the Extraction, Transformation, and Load (ETL) life cycle to topics related to grid search and cross-validation of the model's hyperparameters. Section V presents and discusses the results. Finally, Section VI concludes.

THEORETICAL FRAMEWORK

Wood is one of the most abundant biomaterials on Earth and has been a cornerstone in construction throughout history (Ding et al., 2022). In that way, wood has great potential as a construction material. Nonetheless, it has anisotropic mechanical properties, meaning that its strength changes depending on the grain direction. Besides, the anatomical structure of wood significantly influences its structural properties. Its microstructure considerably impacts parameters such as anisotropy, porosity, density, and mechanical strength (Arriaga et al., 2023). Thus, the mechanical properties of wood primarily depend on the direction in which loads are applied, with significant variation observed between samples from the same wood batch due to different growth conditions and variations in the trunk position during the cutting process. As a cultural and

engineering tradition, wood construction has been passed down through generations, embodying the skills, techniques, and knowledge developed by our ancestors throughout history (Véliz-Fadic et al., 2024). Given its lightness, high strength-to-weight ratio, and aesthetic appeal, wood has seen a greater interest by engineers and architects in the last decades for applications from residential buildings to large-scale commercial projects. The applications of wood in such services have not yet been fully explained concerning the mechanical behavior for various loading conditions based on the resistance parameters that come in compressive, tensile, and shear strengths. The complexities associated with wood's natural variability, including moisture content, species differences, and growth conditions, further complicate its characterization.

The structure of wood can be divided into three levels: macrostructure, microstructure, and sub-microstructure (Niemz & Sonderegger, 2017). Each level directly impacts its mechanical properties (Toumpanaki et al., 2021). Wood is classified as an orthotropic material, which exhibits different mechanical properties along each of its principal axes, i.e., longitudinal, radial, and tangential, which are perpendicular to each other (Fig. 1). To determine its mechanical properties under elastic and inelastic conditions, at least twelve resistance parameters must be identified, including elasticity moduli, shear moduli, and Poisson's ratios, nine of which are independent. However, its structural performance is affected over time by phenomena such as creep and relaxation (Senalik & Farber, 2021).
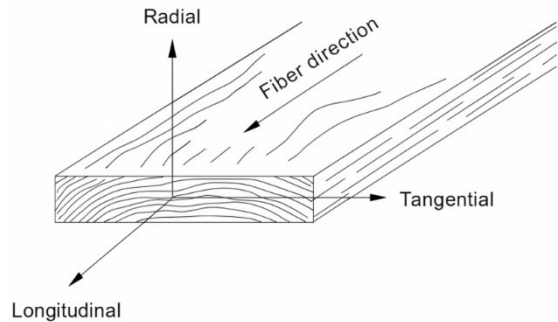
Figure 1. Principal axes of wood of mechanical properties (Senalik & Farber, 2021).

The mechanical properties of wood refer to its ability to withstand loads while maintaining its structural integrity. Determining these properties requires laboratory testing using specialized testing equipment (Record, 1914). To determine the mechanical properties of a wood sample, homogeneous specimens are generally used, preferably free from defects such as knots, cross grains, cracks, or splits. Despite selecting test specimens to be as homogeneous as possible, variations in the obtained mechanical properties may be observed. While this variability is common in most materials used in the construction industry, wood tends to exhibit a high standard deviation (Senalik & Farber, 2021) due to its natural composition, which is influenced by a wide range of external factors that can alter its structure. Due to its cellular composition, wood often exhibits nonlinear behavior, making the parameters for assessing its mechanical performance in this inelastic range more complex (Holmberg et al., 1999). Inelastic behavior factors and changes in moisture content manifest over time as creep and stress relaxation in wood (Senalik & Farber, 2021).

It has been evidenced that density, fiber angle, and ring angle influence the mechanical properties of wood and the microfibril angle. These factors affect properties such as the modulus of elasticity and strength (Arriaga et al., 2023). The apparent density of wood is one of the most influential variables in determining its modulus of elasticity

and mechanical strength. Another parameter that influences wood's mechanical properties and structural behavior is its hygroscopic moisture content. This property allows the wood to exchange moisture with the surrounding air, with values ranging from 30% to over 200% for green wood and below 12% for dry wood (Glass & Zelinka, 2021). Moisture variation in wood, influenced by different drying processes, significantly correlates with its mechanical properties. During adsorption processes, wood conditioned from a dry state exhibits a higher modulus of elasticity and modulus of rupture compared to wood conditioned from a water-saturated state with the same moisture content (Ishimaru et al., 2001). ASTM D198 establishes a standard wood moisture content of 12% for the evaluation of mechanical properties as the standard value for structural wood. This percentage is used to standardize the determination of mechanical properties across most wood species, allowing for comparison between results obtained from different specimens. The 12% value represents the typical hygroscopic equilibrium of wood under average indoor environmental conditions, where its dimensional stability and mechanical properties remain relatively consistent and reliable for structural application (ASTM, 2021). An increase in wood density is directly associated with higher mechanical strength (Soares et al., 2021). In contrast, moisture content has the opposite effect: values below 12% result in low variability in mechanical properties, whereas moisture levels above 12%, particularly those approaching the fiber saturation point (28-30%) lead to a significant reduction in the strength of the wood (Yau et al., 2024).

DATABASE DESCRIPTION

The research was supported by experimental data performed by (Loss, 2023) in which an extended measurement campaign conducted in the Department of Wood Science of the University of British Columbia to determine the mechanical material properties of Canadian small clear spruce-pine-fir wood, widely adopted in North America for constructing cross-laminated timber panels. A total of 690 specimens classified as visually graded No. 2 (sawn wood graded visually based on visible defects like knots, slope of grain or wane), and machine stress-rated 2100fb 1.8E (sawn wood evaluated for structural quality through non-destructive machine). Specimens were tested under compression, tension, and shear loads, in both parallel and perpendicular directions to the grain. The wood test samples were manufactured and treated by a high-precision Homag Centateq P-300 CNC machine to turn the specimens into standardized ones, which would be left in a conditioning room to reach a stable weight with a relative humidity at 20 °C and 65% relative humidity for a period of 15 to 30 days according to the ASTM D143-22 standard to reach a stable weight. Moisture content in test specimens was then measured moisture content using a Sartorius Extend ED6202S-CW digital balance with a precision of 0.01% to be as accurate as possible. Each wood test sample was weighed just before testing. Mechanical tests were carried out using an MTS 810 universal testing machine, and the calibration was performed according to the ASTM E4-01 standard. Other tests performed on the wood include compression and tension parallel and perpendicular to the wood grain, executed at controlled speeds. Real-time data with an acquisition rate of 2 Hz up to the failure of each specimen displays force and deformation. Test results of 690 specimens provide an essential database that will enhance the understanding of the structural performance of Spruce-Pine-Fir and

enable the design and construction of larger-scale structures using this sustainable material.

Table 1. Descriptive statistics of the parallel-to-the-grain experiment

	Mean	Min	Q1	Median	Q3	Max	Std. Dev.
Strain (%)	1.14	0	0.26	1.04	1.88	3.77	0.88
Stress Parallel (MPa)	30.16	0	27.25	32.95	37.93	53.46	11.90

For modeling purposes in the current paper, we present the descriptive statistics of the subsets related to parallel-to-the-grain and perpendicular-to-the-grain stresses and the corresponding strains, as shown in Tables 1 and 2. The results of these tables show a significant difference in the mechanical behavior of the material under these loading conditions. Regarding strain, the perpendicular-to-the-grain experiment shows much higher values according to all statistical measures: the mean value of strain is 4.82% in the case of perpendicular-to-the-grain versus 1.14% in the parallel-to-the-grain case. This means that the material deforms more when loaded perpendicular, supported by the broader range in the experiment for perpendicular, where the maximum strain reached 9.99% compared to 3.77% from the parallel experiment. All these variations are correlated with the anisotropic structure of wood. Its load-bearing capacity varies depending on the direction in which the load is applied and primarily depends on the fiber orientation (Unsal & Candan, 2008). The standard deviation of strain in the perpendicular test was higher, showing more variation in the material's response.

Table 2. Descriptive statistics of the perpendicular-to-the-grain experiment

	Mean	Min	Q1	Median	Q3	Max	Std. Dev.
Strain (%)	4.82	0	2.2	4.79	7.38	9.99	2.95
Stress Perpendicular (MPa)	7.30	0	5.68	7.55	9.19	14.92	2.91

Conversely, the stress values show the opposite behavior. Thus, it can be noticed that the material resists more when loaded parallel to the grain, e.g., the average stress in the parallel experiment is 30.16 MPa compared with the perpendicular direction that achieved up to 7.30 MPa. Also, the interquartile range is more significant in the parallel case because of the increased spread of stress values within the sample. Furthermore, the maximum achieved stress in the parallel direction is higher at 53.46 MPa compared to the maximum of 14.92 MPa in the perpendicular experiment, highlighting the material's superior strength when aligned with the grain. The observed difference between tensile and compressive behavior was expected due to the anatomical differences in wood that result in its anisotropy. Consequently, this difference in strength is significant for the different elastic symmetry axes of wood, making its analytical understanding complex. However, various analytical models theoretically represent this behavior, establishing a possible relationship between wood strength in the principal orthotropic axes (Mascia et al., 2013).

Although different in magnitude, the standard deviations for stress in both directions are relatively consistent proportionally with their respective means, suggesting similar degrees of relative variability in both cases. Overall, data indicate that material is significantly stronger but less deformable when subjected to parallel-to-the-grain loading, whereas it is more compliant but weaker in perpendicular loading
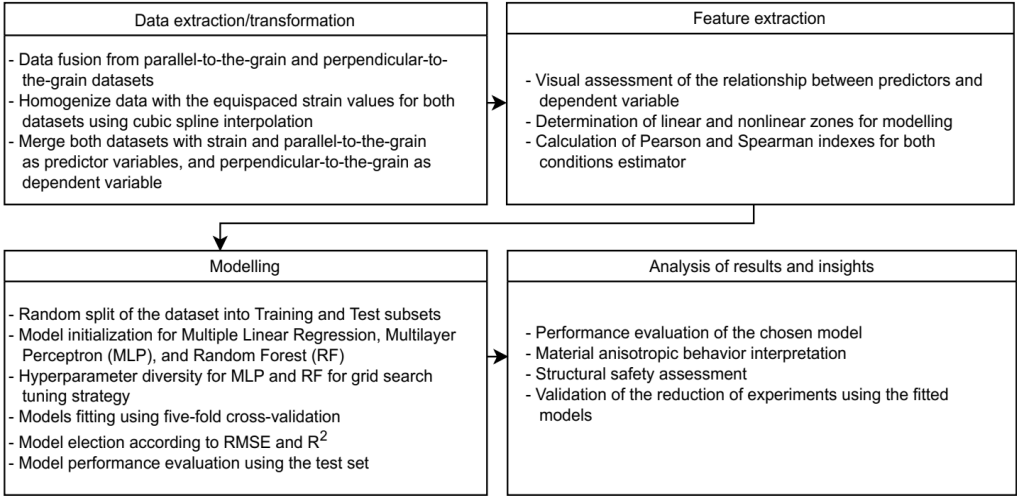
conditions. These differences agree with the expected anisotropic character of wood or similar material, where internal structure confers greater strength in the direction of the grain and flexibility across the grain. Finally, since the dimensions in strain, perpendicular stress, and parallel stress are in different scales, it suggests that we have to homogenize the input data of the proposed models to avoid possible bias.

METHODOLOGY

The process of obtaining the prediction models is depicted in Fig. 2 and comprises four stages. First, we perform the Extraction, Transformation, and Load (ETL) (Khan et al., 2024) to homogenize the data according to the modeling needs. Second, we conduct the feature extraction (Ehtisham et al., 2024) to check the correlations between the predictors and the objective variable. Third, we fit the models. Finally, we analyze the results. The following subsections comprehensively show each stage. Our goal is to find a set of models as

$$\text{Stress}_{\text{per}} = f(\text{Stress}_{\text{par}}, \text{Strain}), \tag{1}$$

where Stress_{per} is the perpendicular-to-the-grain stress, $\text{Stress}_{\text{par}}$ is the parallel-to-the-grain stress, and Strain is the strain.

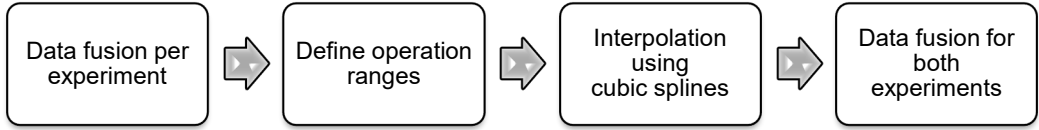| Data extraction/transformation	Feature extraction
- Data fusion from parallel-to-the-grain and perpendicular-to-the-grain datasets - Homogenize data with the equispaced strain values for both datasets using cubic spline interpolation - Merge both datasets with strain and parallel-to-the-grain as predictor variables, and perpendicular-to-the-grain as dependent variable	- Visual assessment of the relationship between predictors and dependent variable - Determination of linear and nonlinear zones for modelling - Calculation of Pearson and Spearman indexes for both conditions estimator
Modelling	Analysis of results and insights
- Random split of the dataset into Training and Test subsets - Model initialization for Multiple Linear Regression, Multilayer Perceptron (MLP), and Random Forest (RF) - Hyperparameter diversity for MLP and RF for grid search tuning strategy - Models fitting using five-fold cross-validation - Model election according to RMSE and R^2 - Model performance evaluation using the test set	- Performance evaluation of the chosen model - Material anisotropic behavior interpretation - Structural safety assessment - Validation of the reduction of experiments using the fitted models

Figure 2. Modeling process.

Data extraction and transformation

The process of data extraction and transformation is depicted in Fig. 3. The first step we followed to obtain the models was to conduct a data fusion between the diverse experiments. The database generally included 43 experiments for parallel-to-the-grain compression and 100 experiments for perpendicular-to-the-grain compression. In that way, the first step was to merge all the data into two files for each experiment. This fusion provides a well-established and repeatable way to capture the behavior of these two standardized experiments to capture the mechanical properties of the wood.

The second step was to limit both experiments to the same strain range since the database characterization shown in Table 1 and Table 2 allowed us to understand that the parallel-to-the-grain campaign was limited to a lower value than the perpendicular-to-the-grain campaign. It was performed to have a uniform range and ease the model fitting phase. In that way, the maximum value of both datasets was 3.77% strain.

Figure 3. Data extraction and transformation.

The third step was to run cubic splines interpolation to have uniform and equispaced rows in both datasets. To this end, we define a range from 0 to 3.77% strain with steps of 0.01%. Cubic spline interpolation approximates smooth, continuous functions through the measurement campaign using cubic polynomials. First, it divides the data points into intervals and fits a cubic polynomial in each interval. These polynomials are determined to satisfy continuity conditions at each given point: continuity of the function, first derivative, and second derivative of the function. To uniquely determine the cubic spline, additional boundary conditions must be imposed. This is commonly accomplished by specifying the second derivative at the endpoints (the natural splines), or the first derivative equals the slope of the data at the ends, which results in clamped splines. The system of equations obtained from these conditions is solved for the coefficients of the cubic polynomials that are then used to interpolate new values within the range and give smooth, accurate approximations of the underlying function. An example of the accuracy of this method is depicted in Fig. 4.
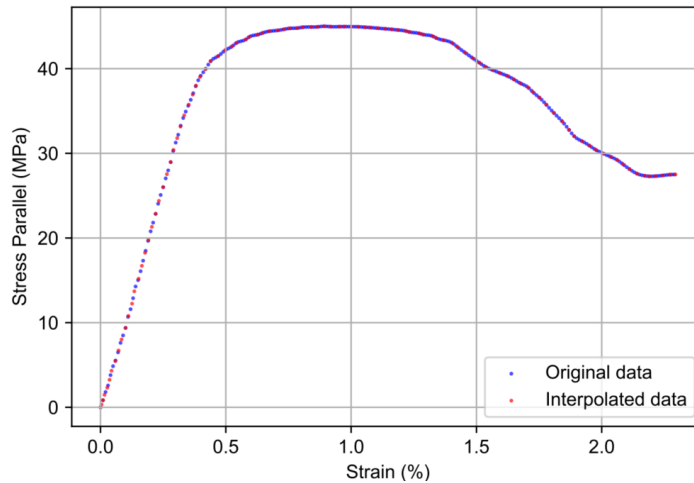
Figure 4. Interpolation process using cubic splines for the first trial of the parallel-to-the-grain experiment. The red curve is the original data, and the blue curve is the interpolated data.

Finally, in the fourth step, we merged the resulting datasets to obtain a three-column database with the variables strain, parallel-to-the-grain stress, and perpendicular-to-the-grain stress.

Feature extraction

The second stage of our framework is determining how the predictor variables correlate with the dependent variable. To this end, we propose the following steps. First, we plotted both independent variables versus the perpendicular-to-the-grain stress to identify linear and nonlinear zones. Then, we delimited these zones to calculate the Pearson and Spearman indices for both zones. The Pearson correlation index helps determine if there are linear relationships between the variables bounded in the interval [-1, 1]. Specifically, *i)* if the values are close to 1, it can be concluded that there is a positive correlation; ii) if the values are close to -1, the correlation is negative; and *iii)* if the values are close to zero, there is no correlation. Furthermore, the Spearman correlation index determines if a nonlinear monotonical function exists to perform regression and can be obtained by ranking the data in ascending order, then assigning a sequential order to each row in the database, subsequently calculating the difference d between the predictor and the dependent variable for each rank; and finally, obtaining the correlation rank ρ.

Modeling

In this section, we propose different parametric and nonparametric models to predict the perpendicular-to-the-grain stress using the results of another experiment (parallel-to-the-grain stress versus strain), improving the time to characterize the wood and reducing the costs associated with the destructive trials.

Multiple linear regression. After obtaining the correlations between the predictors and the dependent variable, we propose a classical Multiple Linear Regression (MLR) model as a baseline to compare the results of different ML-based models. The proposed MLR model is

$$\text{Stress}_{\text{per}} = b_0 + b_1 \text{Strain} + b_2 \text{Stress}_{\text{par}} + \epsilon, \tag{2}$$

where b_0 is the independent term, b_1 is the weight for the Strain, b_2 is the weight for $\text{Stress}_{\text{par}}$, and ϵ is the error that is assumed as independent and identically distributed (i.i.d) zero-mean gaussian variable. The weights' interpretation will help determine the effect of each predictor (positive/negative) on the dependent variable and its relative importance according to the magnitude of the corresponding coefficient.

Artificial neural network. We propose an ANN-based regressor to improve the prediction ability of the fitted models to forecast the perpendicular-to-the-grain stress. In particular, we used a multilayer perceptron (MLP) regression architecture, a type of ANN that aims to approximate complex relationships between the input features and continuous target variables. In the first stage, we apply a max-min scaler to homogenize all the predictor variables in the same orders of magnitude. For instance, the scalization of the ith sample of the strain variable can be calculated as

$$\text{Strain}_i = \frac{\text{Strain}_i - max(\text{Strain})}{max(\text{Strain}) - min(\text{Strain})} \tag{3}$$

The exact process is performed for the variable $\text{Stress}_{\text{per}}$. The scaling process must be performed to avoid a specific variable dominating the other due to the difference in

magnitudes. The architecture of an MLP includes an input layer, one or more hidden layers, and an output layer, as shown in Fig. 5. In our case, we have two input neurons (Strain and Stress$_{par}$), a set of n hidden layers with different numbers of neurons h$_{ij}$ (where i indicates the number of the hidden layer and j indicates the neuron number of the corresponding layer), and an output layer (Stress$_{per}$). The number of neurons in each hidden layer is an essential hyperparameter since it influences the capability of the model to learn the pattern of the data directly, so it is mandatory to find the most suitable configuration through hyperparameter tuning.
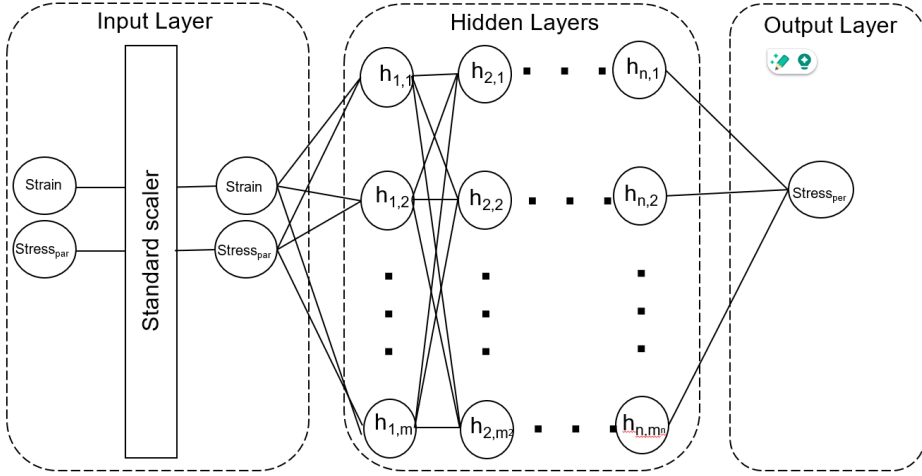

Figure 5. Multilayer Perceptron Architecture for the regressor.

The neurons h$_{ij}$ are part of the fundamental computing unit. They receive weighted inputs, with an activation function applied to an output propagating to subsequent layers. Each neuron sums all the inputs based on an optimized weight, adds a bias, and transforms the obtained calculation using an activation function that introduces the non-linearity needed to learn complex relationships. We used the rectified linear unit (ReLU) activation function due to its computational efficiency and involvement in preventing vanishing gradient problems. Furthermore, we varied different learning rates since this hyperparameter regulates the optimization algorithm's step size for updating the model weights during backpropagation. The learning rate is a crucial hyperparameter since too high values cause the model to oscillate around an optimal solution, and too low values generate slow or suboptimal convergence. Often, the choice of learning rate is empirical or dynamically adjusted during training using optimization strategies that adaptively modify the learning rate, such as Adam or Stochastic Gradient Descent (SGD). In that way, we generated a grid varying the MLP architecture regarding the number of hidden layers, the number of neurons per layer, the learning rate values, and the adaptative algorithm to adequately balance the learning rate variation.

Once the hyperparameters grid is configured, we divide the dataset into training and test sets. This split was performed with a proportion of 80% for training and 20% for testing. We used the training set to find how a particular configuration of hyperparameters learns the patterns and measure the goodness-of-fit using the Root Mean Square Error (RMSE) for the corresponding network configuration. Furthermore,

we implemented a five-fold cross-validation strategy as follows. First, we divided the training set into five subsets, namely S_1, S_2, S_3, S_4, and S_5. Then, we trained with four subsets, e.g., S_1, S_2, S_3, and S_4, and measured the RMSE with S_5. Subsequently, we performed the same procedure, varying the subset to calculate the RMSE; that is, we trained four models with the same hyperparameters. Finally, with the obtained RMSEs, we calculated the standard deviation to assess the generalization ability of each configuration. We chose the hyperparameters which exhibited the lowest RMSE and best R^2. With the fitted MLP model, we used the test set to find the RMSE and R^2 to assess how the fitted model performs in the presence of unknown data.

Random Forest. We fitted a Random-Forest-based model to improve the accuracy in the prediction of the perpendicular-to-the-grain stress, as depicted in Fig. 6. From that figure, it can be noticed that this architecture has different stages, from the scalization of the variables, the regression using Decision Trees (DTs), and the aggregation of the prediction of the DTs to obtain the final prediction.
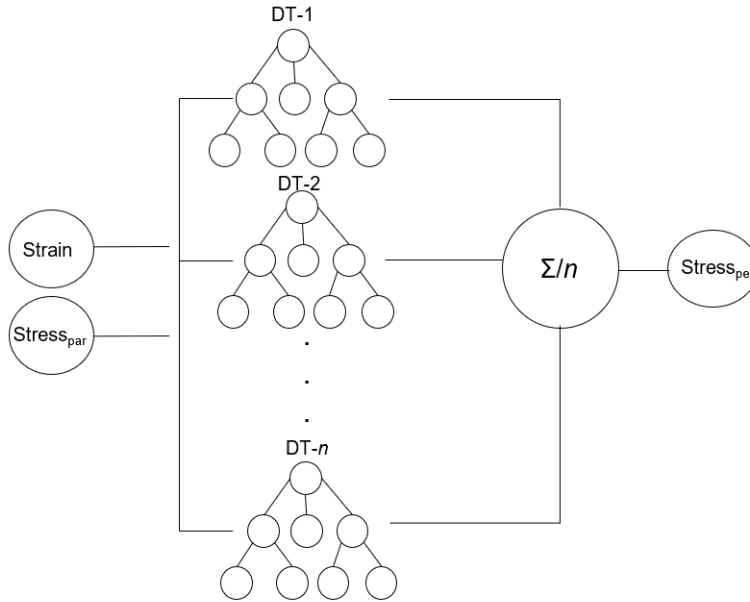
Figure 6. Random Forest architecture.

Subsequently, we train a set of n DTs. The DTs are machine-learning strategies that can be used for regression using the Classification and Regression Trees (CART) algorithm. The operation principle behind the CART algorithm is to partition the input space recursively into different regions to minimize a cost function based on the Mean Square Error (MSE). To this end, the algorithm CART computes all the possible partitions for the predictor variables, calculates the MSE for each, scores the partitions, sorts them to find the lowest MSE, and configures a set of nested if-else clauses verifying if the current value of the predictor variables meets any of the criteria in the conditionals. The partitions finish when a stop criterium is met, like the number of nested conditionals (number of branches) or the minimum number of points per each conditional (number

of leaves per branch). Both stop criteria are hyperparameters for this strategy and must be fine-tuned using grid search and cross-validation, as previously discussed in the MLP section. Finally, the DT delivers the mean of the values for the corresponding region.

However, the DTs are prone to cause overfitting, an undesirable balance between the prediction performance when the training is performed, usually high, versus the performance when the test set is used, usually low. Because of that, a set of n DTs is fitted using bootstrapping and aggregation (bagging), as shown in Fig. 6. Thus, the bootstrapping randomly splits the training set using fewer rows and augments the size of the corresponding subsets, repeating some rows. Each DT uses a different subset to incorporate a random character into the random forest. Finally, the results of all the DTs are aggregated by computing the mean of each prediction. The value for n is also a hyperparameter that has to be fine-tuned using grid search and cross-validation.

RESULTS AND DISCUSSION

In this section, we present the results of the feature extraction stage, where we determined if the predictor variables could predict the dependent variable's variability. After fitting all the proposed models in Section III, we present the obtained models and performance metrics.

Feature extraction

The first step to validate the relationships between the predictor variables and the perpendicular-to-the-grain stress was to plot the different trials for the same experiments. Figs 7 and 8 provide a graphical compilation of all the original data used in the analysis conducted in this study. They highlight the contrast in data behavior when plotting the stress–strain relationship (Fig. 7) versus the relationship between stresses perpendicular and parallel to the grain (Fig. 8).
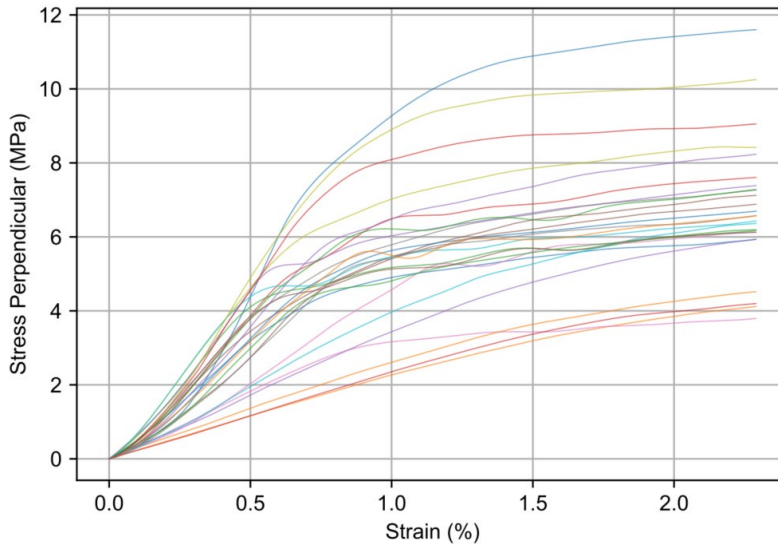
Figure 7. Trends for different trials for perpendicular-to-the-grain stress versus strain and.

For the case of Fig. 8, the following conclusions can be drawn. First, it can be noticed that there is a linear region for each trial that exhibits the elastic material behavior, i.e., when the load is applied and subsequently released, and when the wood can recover the original shape without alterations. This linear relationship is maintained up to strain values close to 0.5% for the higher-strength samples, and up to approximately 1% for the lower-strength specimens. It can also be noticed that there is a nonlinear region, i.e., an inelastic region, where the wood cannot recover its original shape after a load-release operation, and after the unloading of the structural element, permanent residual deformations remain. Although there is a clear relationship between the strain and the perpendicular-to-the-grain stress, we can remark that there is considerable variability among the diverse trials since some of them stabilize at 4 MPa while the most resistant stabilize within the range of 6 MPa to 12 MPa. These variations are associated with the specimen's heterogeneity, caused mainly by grain orientation, density, moisture content, and natural defects like knots or fiber misalignment. Specifically, it can be noticed that this variability does not follow a single universal pattern. In that way, machine-learning-based models can predict this nonlinear behavior and capture the variability efficiently.
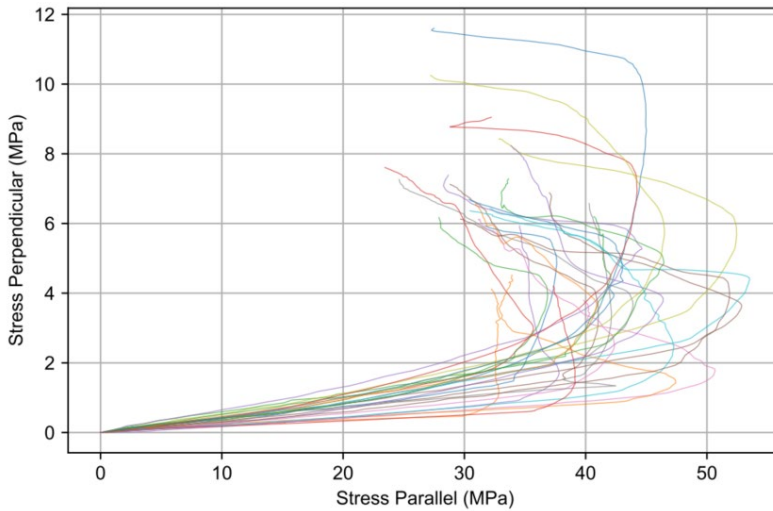
Figure 8. Trends for different trials for perpendicular-to-the-grain stress versus parallel-to-the-grain stress.

This accurate prediction of material behavior in both its linear elastic range and plastic performance region provides a significant advantage of Machine Learning over traditional analytical and numerical finite element models commonly used to predict the structural performance of various materials, including wood. The nonlinear behavior of materials is primarily influenced by parameters such as plasticity, anisotropy, and material defects, which are, in most cases, complex to model using conventional mathematical approaches.

In addition, the following can be noticed in Fig. 8, which presents the trend between the perpendicular-to-the-grain stress versus the parallel-to-the-grain stress. First, a relatively linear trend is presented, where a proportional increase as the parallel-to-the-

grain stress increases. All specimens, regardless of their maximum load-bearing capacity, exhibit linear elastic behavior up to approximately 30 MPa of stress parallel to the wood grain. Again, this behavior corresponds to the elastic region where the material deforms predictably under different loads. Nonetheless, the curves become highly nonlinear as the predictor variable increases, exhibiting a complex and scattered distribution. Since wood is an anisotropic material, the microstructural failures become noticeable, mainly explained by different phenomena like cracking, fiber buckling, and delamination. Furthermore, the same effect of high variability in different specimens is presented due to differences in moisture content and density, among others. Finally, the nonlinear behavior can also be attributed to the microcracks and shear deformations caused when the parallel-to-the-grain load is applied, affecting the perpendicular-to-the-grain stress. Machine Learning algorithms, deep learning models, and regression techniques may identify highly complex patterns in the mechanical behavior of wood under different stress conditions. This capability may enable accurate predictions of wood behavior under both parallel and perpendicular loading to the fiber. These models efficiently handle large volumes of data, perform multivariable analysis, and adapt to different behavioral models to effectively predict mechanical properties, failure mechanisms, and long-term performance of materials such as wood with high precision.

The nonlinear relationship between stress and strain shown in Fig. 7 exhibits a trend with a stable and well-defined transition. In contrast, Fig. 8 shows that the nonlinear relationship between stress perpendicular to the grain and stress parallel to the grain does not follow a clear pattern, as each test displays an independent behavior. Despite the observed nonlinearity in both the stress-strain relationship and the interaction between parallel and perpendicular grain stresses, machine learning techniques can effectively predict the mechanical behavior of wood in the perpendicular-to-grain direction based on its structural performance in the parallel-to-grain direction.

On the other hand, we used the Pearson and Spearman indices to determine the relationship among the strain, the parallel-to-the-grain stress, and the perpendicular-to-the-grain stress, as shown in Table 3, from the following can be noticed. First, both indices show that the strain influences the perpendicular-to-the-grain stress,

Table 3. Correlations between predictor variables and the perpendicular-to-the-grain Stress. We used the Pearson correlation factor R^2 and the Spearman index ρ

	R^2 (%)	ρ (%)
Strain (%)	0.58	0.62
Stress Parallel (MPa)	0.299	0.52

particularly on the other hand, we used the Pearson and Spearman indices to determine the relationship among the strain, the parallel-to-the-grain stress, and the perpendicular-to-the-grain stress, as shown in Table 3, from the following can be noticed. First, both indices show that the strain influences the perpendicular-to-the-grain stress, particularly in the elastic zone, where a simple linear regression can be effective and computationally inexpensive to predict this variable. Nonetheless, the inelastic region, characterized by a nonlinear behavior, shows that the parallel-to-the-grain could be used to find a monotonic parametric or nonparametric function to improve the quality of the prediction. In that way, both variables contribute to predicting the variability of the dependent variable and validate our hypothesis previously depicted in Eq. (1).

Multiple linear regression model

The following stage of the proposed framework was fitting the different parametric and nonparametric models. To this end, we randomly divided the collected data into training and test sets with a proportion of 80%–20%, using the Python library sklearn.model_selection and the method train_test_split. Subsequently, we fitted the model in Eq. (2) and found the coefficients and 95% Confidence Intervals (CIs) shown in Table 4. Our modeling was conducted for the elastic region, where the parallel-to-the-grain stress is less than 30 MPa, and the strain is less than 0.8% since the results from Table 3 and Fig. 7 showed that an MLR model could be suboptimal in the inelastic region. Notice that the independent term obtained a value of -0.296 MPa with a CI in the range [-0.473, -0.121]. This suggests that when no loads are parallel or perpendicular, the load has a slightly negative value, which can be attributed to a measurement error without a physical interpretation. Regarding b_1, note that a 1% increase in the strain means that the perpendicular-to-the-grain stress also increases by 3.411 MPa, which is expected for this material that is prone to deflect due to its nature. Besides, the narrow confidence interval shows that this variable adequately approximates the dependent variable behavior. Besides, the estimation for b_2 suggests that for 1 MPa increase in the parallel-to-the-grain stress, an increase of 0.042 MPa occurs in the dependent variable.

Table 4. Coefficients and 95% CIs for the MLR model

Variable	Symbol	Value	95% CI	Units
Independent term	b_0	-0.296	[-0.473, -0.121]	MPa
Strain (%)	b_1	3.411	[3.297, 3.526]	MPa/%
Stress Parallel (MPa)	b_2	0.042	[0.031, 0.052]	Adim

This value can be explained since a more pronounced deformation arises in parallel deformation, while perpendicular behavior is more resilient under stress conditions. This behavior is primarily due to the anisotropic structure of wood and the arrangement of its cells, which influence how stresses are transmitted within the material's internal structure. Since the cellulose fibers are aligned parallel to the applied load, stress transmission occurs efficiently without significant interruptions. In contrast, in the perpendicular direction, wood exhibits lower load-bearing capacity due to its anatomical structure. The application of load in this direction tends to separate the fibers, leading to faster failure. In the same way, the narrow confidence interval suggests that this variable accurately predicts the perpendicular-to-the-grain stress in the elastic zone.

On the other hand, we present the numerical performance of the fitted MLR model in Table 5. Notice that the results of the training and test sets are similar, indicating that the model has adequate generalization ability and a low risk of overfitting. Regarding the

Table 5. MLR model performance for training and test sets

Subset	R^2	RMSE (MPa)
Training	0.909	1.039
Test	0.916	1.036

R^2 and the RMSE, the model can explain about 91% of the variability of the wood behavior and exhibit about 1 MPa of error for the elastic zone, indicating that for normal operational conditions, an MLR-based model is a computationally effective and highly interpretable model, even considering that wood is anisotropic and depends on uncontrollable variables like moisture and density.

Artificial neural network

We fitted the MLP-based regression model in Fig. 5 using the library sklearn.neural_network and the class MLPRegressor. First, we used the same database split described in the previous section, with 80%–20% proportion. However, our aim in fitting this model is to find a regressor that can accurately forecast the elastic and inelastic regions, different from the MLR-based model that was fitted only for the elastic region. In that way, we conducted a grid search and cross-validation to find the best configuration to achieve the lowest bias, variance, RMSE, and the highest R^2. The summary of the hyperparameters is shown in Table 6. Specifically, we tested the following network architectures: *i)* a single hidden layer with 50 neurons, *ii)* a single layer with 100 neurons, and *iii)* two hidden layers with 50 neurons in each layer. Regarding the activation function responsible for introducing the nonlinear behavior to the regressor, we tested the ReLU and hyperbolic tangent options since they are commonly used for regression tasks. Regarding the learning rate, we used a static strategy with values of 0.0001 and 0.01, aiming to have slow and fast responses in convergence. Furthermore, we also set a dynamic scheme to adjust the network weight updates using well-known algorithms like Adam and SGD. Finally, we performed the five-fold cross-validation scheme to avoid overfitting, controlling the standard deviation of the fitted models. In that way, we tested three network configurations, two activation functions, two learning rates, two weight optimizers, and five-fold cross-validation, so we trained 120 models.

**Table 6.** Hyperparameter ranges and best configurations for the MLP model

Hyperparameter	Configurations tested	Best configuration
Network architecture	(2, 50, 1), (2, 100, 1), (2, 50, 50, 1)	(2, 50, 50, 1)
Activation functions	ReLU, hyperbolic tangent	ReLU
Learning rate	0.0001 and 0.01	0.0001
Optimizer	Adam and SGD	Adam

The best model achieved the results shown in Table 7 using the following configuration: *i)* a ReLu activation function, *ii)* a learning rate of 0.0001, *iii)* a network architecture with two layers with 50 neurons per layer, and *iv)* the weight optimizer Adam. With the selected configuration, the following observations can be drawn. First, the MLP-based achieved a considerably high R^2 when comparing the predictions versus the actual data from the test subset since we achieved a capacity to predict variability up to 70% compared to the obtained correlations up to 0.62 in Table 3, which denotes a noticeable improvement of the nonparametric machine-learning-based regressors to learn nonlinear patterns like those exhibited by the anisotropic behavior of wood. Besides, the standard deviation of the cross-validation process was 0.104 MPa, a relatively negligible value considering the high variability of the material. Finally, the RMSE ranges from 1.3 to 1.4 MPa, which can be high considering the scale of the experiments. However, a visual exploration

Table 7. MLP-based model performance for training and test sets considering elastic and non-elastic regions. The training includes the standard deviation s to show the model's generalization ability

Subset	R^2	RMSE (MPa)
Training	0.729	1.311, $s = 0.104$
Test	0.708	1.378

performed in Fig. 9. showed that the MLP-based regressor can predict with acceptable accuracy the behavior of the dependent variable when using the strain and the parallel-to-the-grain stress. Although these results seem less accurate than those obtained by the MLR-based model, it is essential to note that this model was fitted to predict the material performance in the inelastic zone, which is highly variable.

(a) Trial 9   (b) Trial 15   (c) Trial 21
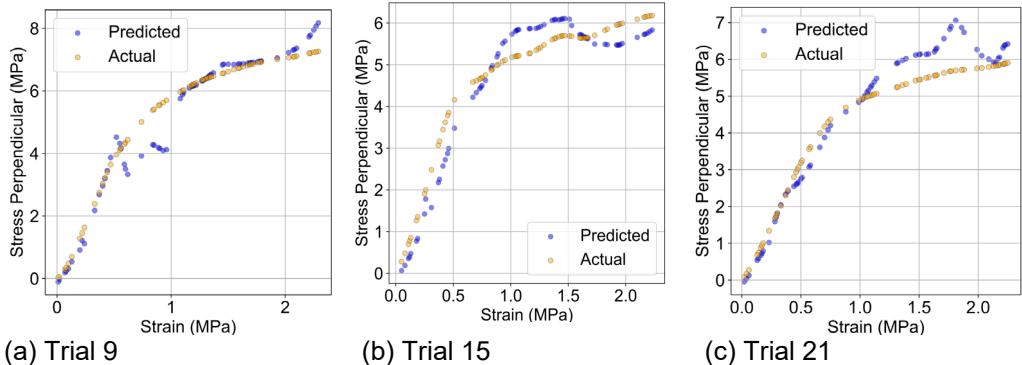
Figure 9. Prediction of the perpendicular-to-the-grain stress versus strain for some experiment trials using the MLP-based model. The dark purple scatters represent the actual data, and the blue scatters represent the predictions.

Random forest

The last model we fitted was based on the Random Forest according with the architecture presented in Fig. 6 using the library sklearn.ensemble and the class RandomForestRegressor. As discussed in the previous section, we kept the same database split into 80%–20% proportions for the training and test sets. We also performed the grid search and five-fold cross-validation procedures to preserve low bias, variance, and high accuracy. In the same way as the MLP-based regressor, we aimed to predict the behavior of the perpendicular-to-the-grain stress based on the elastic and inelastic zones. The summary of the considered hyperparameters is shown in Table 8.

Table 8. Hyperparameter ranges and best configurations for the RF model

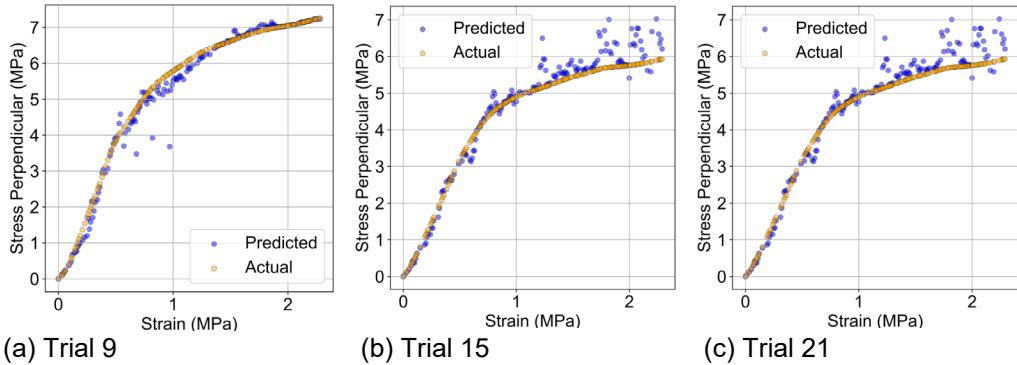| Hyperparameter	Configurations tested	Best configuration
Forest size	50, 100, 200	100
Tree Depth	No restriction, 10, 20	10
Min number of simples per split	2, 5, 10	5

Specifically, we tested different forest sizes, with values of 50, 100, and 200 trees in the forest. Regarding the trees' depths, we limited the DTs with no restrictions and constrained this hyperparameter to 10 and 20 levels. This configuration allowed us to examine how deeper trees influence the model's performance regarding overfitting. Finally, we also varied the hyperparameter related to the minimum number of samples required to split a node with values of 2, 5, and 10, ensuring that these settings allow the trees to grow sufficiently while preserving the generalization capacity of the random forest. Since we set three different forest sizes, three tree depths, and three values for the minimum number of samples per split and used five subsets for the cross-validation process, we trained a total of 135 models. The selected model was the one that provided

the best tradeoff between accuracy and generalization, aiming to capture the linear and nonlinear behavior of the perpendicular stress of the wood.

The best model achieved the results in Table 9 using the following configuration: *i)* a forest size of 100 DTs, *ii)* a tree depth of 10, and *iii)* a minimum number of samples to split a node of 5. From this table, it can be noticed that the RF-based model achieved the best performance compared to the MLP-based model and the MLR model since it could predict the data variability up to 91% in the test set; that is, our fitted model could adequately forecast the inelastic behavior of the wood in the perpendicular-to-the-grain stress when using the strain and the parallel-to-the-grain stress. Note also that the RMSE achieved was considerably lower than

Table 9. RF-based model performance for training and test sets considering elastic and non-elastic regions. The training includes the standard deviation s to show the model's generalization ability

Subset	R^2	RMSE (MPa)
Training	0.95	0.58, $s = 0.082$
Test	0.91	0.62

that obtained using the MLP-based regressor with values up to 0.62 MPa. Finally, the standard deviation was 0.082 MPa, indicating an adequate generalization ability of the model in the presence of unknown data. The visual exploration of some experiment trials in Fig. 10 confirms the fitted model's accuracy since most predicted values are close to the actual ones when using the test set.

(a) Trial 9   (b) Trial 15   (c) Trial 21

Figure 10. Prediction of the perpendicular-to-the-grain stress versus strain for some experiment trials using the RF-based model. The orange scatters represent the actual data, and the blue scatters represent the predictions.

CONCLUSIONS

This study showed how machine learning techniques can enhance the prediction of mechanical behavior in wood, a sustainable construction material that is becoming increasingly important in engineering. Conventional modeling approaches in the characterization of wood, like multiple linear regression, have demonstrated a lack of capability in representing nonlinear and anisotropic material properties, particularly in the inelastic region. We further proposed applying ANN and RF models to balance interpretability and computational complexity in improving predictive accuracy and generalization capability. The MLR model, computationally efficient and interpretable,

showed an adequate performance for the elastic region but limited capabilities for the inelastic zone. The MLP-based model was trained using hyperparameter tuning with cross-validation to result in a better nonlinear relationship capture capability, especially around the transition between elastic and inelastic behavior. While this provided a higher capability in learning complex patterns, the model had higher RMSEs: 1.31 MPa for training and 1.38 MPa for testing. That may indicate that neural networks are struggling with wood's inherently variable and anisotropic nature and could require more extensive feature engineering or larger datasets to achieve optimal performance. However, the random forest model had the best performance among all three techniques, with the most generalizable and closest predictions in elastic and inelastic regions. Giving a high R^2 of 0.95 for training and 0.91 for testing, with a significantly lower RMSE at 0.58 MPa for training and 0.62 MPa for testing, the RF-based approach showed the best adaptability to learn linear and nonlinear behaviors. It also seemed that the variance in this model, when cross-validated, was relatively low, pointing toward its robustness and strong generalization capabilities. This result now points toward ensemble learning, especially tree-based models, for modeling such mechanical responses for complicated materials like wood.

As expected, the data observed in the experimental tests show a strong correlation that can be predicted using ML-based models. This prediction of the main mechanical properties along the different anisotropic axes is primarily attributed to the anatomy of the wood, which consists mainly of elongated cells organized in a predominant direction. The orientation of these cells plays a crucial role in determining the structural performance of the material. Although the fitted models achieved an adequate prediction capacity with high accuracy, this research also outlines essential conclusions regarding wood characterization and sustainable construction since it showed that the use of machine learning techniques can reduce the need for extensive experimental setups and campaigns, reducing the associated costs, since the experiments associated with the perpendicular-to-the-grain stress can be forecasted using a different experiment, in this case, the characterization of the parallel-to-the grain stress versus the strain. These findings can be extrapolated for different structural methodologies with high reliability in civil engineering.

USE OF GENERATIVE AI DECLARATION. The authors confirm that they used ChatGPT to fix typo errors, improve grammar, translate some excerpts from Spanish, and enhance the readability of the manuscript. However, they declare that the manuscript is original, and the improved texts obtained from the language models have been carefully reviewed.

REFERENCES

Arriaga, F., Wang, X., Íñiguez-González, G., Llana, D.F., Esteban, M. & Niemz, P. 2023. Mechanical properties of wood: A review. *Forests* **14**(6), 1202. doi: 10.3390/f14061202

ASTM International. 2021. ASTM D198-21: Standard Test Methods of Static Tests of Lumber in Structural Sizes. West Conshohocken, PA: ASTM International. https://doi.org/10.1520/D0198-21

ASTM International. 2021. ASTM D5457-21a Standard Specification for Computing Reference Resistance of Wood-Based Materials and Structural Connections for Load and Resistance Factor Design. West Conshohocken, PA: ASTM International. doi: 10.1520/D5457-21A

Ding, Y., Pang, Z., Lan, K., Yao, Y., Panzarasa, G., Xu, L., Lo Ricco, M., Rammer, D.R., Zhu, J.Y. & Hu, M. 2023. Emerging engineered wood for building applications. *Chemical Reviews* **123**(5), 1843–1888. https://doi.org/10.1021/acs.chemrev.2c00588

Ehtisham, R., Qayyum, W., Camp, C.V., Plevris, V., Mir, J., Khan, Q.Z. & Ahmad, A. 2024. Computing the characteristics of defects in wooden structures using image processing and CNN. *Automation in Construction* **158**, 105211. doi: 10.1016/j.autcon.2023.105211

Giraldo, J.M.G. & Palacio, L.G. 2020. The fourth industrial revolution, an opportunity for Civil Engineering. *2020 15th Iberian Conference on Information Systems and Technologies (CISTI)*, 1–7. https://doi.org/10.23919/CISTI49556.2020.9141138

Glass, S.V. & Zelinka, S.L. 2021. Moisture relations and physical properties of wood. In *Wood Handbook—Wood as an Engineering Material* (FPL-GTR-282), Chap. 4, 4–1–4–22.

Gonzalez-Palacio, M., Moncada, S.V., Luna-delRisco, M., Gonzalez-Palacio, L., Montealegre, J.J.Q., Orozco, C.A.A., Diaz-Forero, I., Velasquez, J.-P. & Marin, S.-A. 2018. Internet of things baseline method to improve health sterilization in hospitals: An approach from electronic instrumentation and processing of steam quality. *2018 13th Iberian Conference on Information Systems and Technologies (CISTI)*, 1–6. https://doi.org/10.23919/CISTI.2018.8398648

González-Palacio, M., Tobón-Vallejo, D., Sepúlveda-Cano, L.M., Luna-delRisco, M., Roehrig, C. & Le, L.B. 2024. Machine-Learning-Assisted Transmission Power Control for LoRaWAN Considering Environments With High Signal-to-Noise Variation. *IEEE Access* **12**, 54449–54470. https://doi.org/10.1109/ACCESS.2024.3387457

Holmberg, S., Persson, K. & Petersson, H. 1999. Nonlinear mechanical behaviour and analysis of wood and fibre materials. *Computers & Structures* **72**(4–5), 459–480. https://doi.org/10.1016/S0045-7949(98)00331-9

Ishimaru, Y., Arai, K., Mizutani, M., Oshima, K. & Iida, I. 2001. Physical and mechanical properties of wood after moisture conditioning. *Journal of Wood Science* **47**, 185–191. https://doi.org/10.1007/BF01171220

Khan, B., Jan, S., Khan, W. & Chughtai, M.I. 2024. An overview of ETL techniques, tools, processes and evaluations in data warehousing. *Journal on Big Data* **6**(1), 1–20. https://doi.org/10.32604/jbd.2023.046223

Kim, J.-H., Park, W.-G. & Kim, N.-H. 2024. Performance of convolutional neural network (CNN) and performance influencing factors for wood species classification of *Lepidobalanus* growing in Korea. *Scientific Reports* **14**(1), 18141. doi: 10.1038/s41598-024-69281-y

Kumar, R., Gupta, S.K., Wang, H.-C., Kumari, C.S. & Korlam, S.S.V.P. 2023. From efficiency to sustainability: Exploring the potential of 6G for a greener future. *Sustainability* **15**(23), 16387. https://doi.org/10.3390/su152316387

Loss, C. 2023. Experimental campaign on the mechanical properties of Canadian small clear spruce-pine-fir wood: Experimental procedures, data curation, and data description. *Data in Brief* **48**, 109064. https://doi.org/10.1016/j.dib.2023.109064

Mascia, N.T., Todeschini, R. & Nicolas, E.A. 2013. Criterion assessment of strength of anisotropic materials applied to wood using uniaxial and biaxial tests. *Revista Sul-Americana de Engenharia Estrutural* **10**(2), 5–30 (in Portuguese).

Niemz, P. & Sonderegger, W. 2017. *Holzphysik: Physik des Holzes und der Holzwerkstoffe* [Wood physics: Physics of wood and wood-based materials]. München: Carl Hanser Verlag. 580 pp. (in German). https://doi.org/10.3139/9783446445468

Palacio, M.G., Palacio, L.G., Montealegre, J.J.Q., Pabón, H.J.O., Del Risco, M.A.L., Roldán, D., Salgarriaga, S., Vásquez, P., Hernández, S. & Martínez, C. 2017. A novel ubiquitous system to monitor medicinal cold chains in transportation. *2017 12th Iberian Conference on Information Systems and Technologies (CISTI)*, 1–6. doi: 10.23919/CISTI.2017.7975685

Peng, L., Searchinger, T.D., Zionts, J. & Waite, R. 2023. The carbon costs of global wood harvests. *Nature* **620**(7972), 110–115. https://doi.org/10.1038/s41586-023-06187-1.

Record, S.J. 1914. *The mechanical properties of wood: Including a discussion of the factors affecting the mechanical properties, and methods of timber testing*. New York, NY: John Wiley & Sons, 165 pp.

Rodríguez-Grau, G., Marín-Uribe, C.R., García-Giraldo, J.M. & Estay, C. 2022. Flexural strength characterisation of oblique radiata pine splice joints. *Wood Material Science & Engineering* **17**(6), 1010–1019. https://doi.org/10.1080/17480272.2021.1990405

Senalik, C.A. & Farber, B. 2021. Mechanical properties of wood. In *Wood Handbook—Wood as an Engineering Material* (FPL-GTR-282), Chap. 5: pp. 5–1; 5–44.

Sharma, A., Garg, S. & Sharma, V. 2024. ATR-FTIR spectroscopy and machine learning for sustainable wood sourcing and species identification: Applications to wood forensics. *Microchemical Journal* **200**, 110467. https://doi.org/10.1016/j.microc.2023.110467

Soares, L.S.Z.R., Fraga, I.F., de Souza e Paula, L., Arroyo, F.N., Ruthes, H.C., de Moura Aquino, V.B., Molina, J.C., Panzera, T.H., Branco, L.A.M.N., Chahud, E., Christoforo, A.L. & Lahr, F.A.R. 2021. Influence of moisture content on physical and mechanical properties of *Cedrelinga catenaeformis* wood. *BioResources* **16**(4), 6758–6765.

Toumpanaki, E., Shah, D.U. & Eichhorn, S.J. 2021. Beyond what meets the eye: Imaging and imagining wood mechanical–structural properties. *Advanced Materials* **33**(28), 2001613. https://doi.org/10.1002/adma.202001613

Unsal, O. & Candan, Z. 2008. Moisture content, vertical density profile and Janka hardness of thermally compressed pine wood panels as a function of press pressure and temperature. *Drying Technology* **26**(9), 1165–1169. https://doi.org/10.1080/07373930802266306

Véliz-Fadic, F.I., Rodríguez-Grau, G., Marín-Uribe, C.R., García-Giraldo, J.M., González-Palacio, L. & Araya-Letelier, G. 2024. Flexural performance assessment of the effect of the splice length of the Jupiter ray type made of radiata pine using computer-aided design and computer-assisted manufacturing. *Construction and Building Materials* **449**, 138272. https://doi.org/10.1016/j.conbuildmat.2024.138272

Yan, X. & Su, X. 2009. *Linear regression analysis: Theory and computing*. Singapore: World Scientific, 348 pp.

Yau, Y., Sulaiman, T.A., Baba, Z.B., Amartey, B.H.S., Sabari, A.A. & Garba, I. 2024. Influence of density and moisture content on the compressive strength parallel to grain of *Gmelina arborea* timber specie. In *Proceedings of the 12th Annual and International Conference of the Renewable and Alternative Energy Society of Nigeria (RAESON)*, Wudil, Kano State, Nigeria, 2–5 June 2024, 1–12.